



## Article

# Assessing the Recent Trends of Land Degradation and Desertification in Romania Using Remote Sensing Indicators

Irina Ontel <sup>1,\*</sup> , Sorin Cheval <sup>2,3,4</sup> , Anisoara Irimescu <sup>1</sup> , George Boldeanu <sup>5</sup>, Vlad-Alexandru Amihaesei <sup>3,6</sup> , Denis Mihailescu <sup>1</sup> , Argentina Nertan <sup>1</sup> , Claudiu-Valeriu Angearu <sup>1</sup> and Vasile Craciunescu <sup>1</sup>

- <sup>1</sup> Remote Sensing and Satellite Meteorology Laboratory, National Meteorological Administration, 97 Sos. București-Ploiești, 013686 Bucharest, Romania; anisoara.irimescu@meteoromania.ro (A.I.); denis.mihailescu@meteoromania.ro (D.M.); argentina.nertan@meteoromania.ro (A.N.); claudiu.angearu@meteoromania.ro (C.-V.A.); vasile.craciunescu@meteoromania.ro (V.C.)
- <sup>2</sup> National Institute for Research and Development in Forestry “Marin Dracea”, 077190 Bucharest, Romania; sorin.cheval@meteoromania.ro
- <sup>3</sup> Department of Climatology, National Meteorological Administration, 97 Sos. București-Ploiești, 01686 Bucharest, Romania; vlad.amihaesei@meteoromania.ro
- <sup>4</sup> Faculty of Geography, Doctoral School of Geography, Babeș-Bolyai University, 5-7 Clinicilor Street, 400347 Cluj-Napoca, Romania
- <sup>5</sup> Faculty of Geography, Doctoral School “Simion Mehedinți”, University of Bucharest, Blvd. Nicolae Bălcescu, no.1, 030018 Bucharest, Romania; george.boldeanu20@gmail.com
- <sup>6</sup> Department of Geography, Faculty of Geography and Geology, Alexandru Ioan Cuza University of Iași, 20A Carol I Blvd., 700505 Iași, Romania
- \* Correspondence: irina.ontel@meteoromania.ro



**Citation:** Ontel, I.; Cheval, S.; Irimescu, A.; Boldeanu, G.; Amihaesei, V.-A.; Mihailescu, D.; Nertan, A.; Angearu, C.-V.; Craciunescu, V. Assessing the Recent Trends of Land Degradation and Desertification in Romania Using Remote Sensing Indicators. *Remote Sens.* **2023**, *15*, 4842. <https://doi.org/10.3390/rs15194842>

Academic Editors: Jie Wang, Xinxin Wang, Yongchao Liu and Xiaocui Wu

Received: 1 September 2023  
Revised: 29 September 2023  
Accepted: 3 October 2023  
Published: 6 October 2023



**Copyright:** © 2023 by the authors. Licensee MDPI, Basel, Switzerland. This article is an open access article distributed under the terms and conditions of the Creative Commons Attribution (CC BY) license (<https://creativecommons.org/licenses/by/4.0/>).

**Abstract:** Land degradation (LD) and desertification (DS) are a sensitive global issue including southern and south-eastern Europe, which is severely affected by climate change. In this study, a state-of-the-art approach for assessing the intensity of LD and DS processes using remote-sensing-derived indicators within a GIS environment was proposed. The analysis was carried out using the Principal Component Analysis based on integrating the significant trends of relevant biophysical parameters in Romania. The methodology was tested and validated at the national level in Romania. In total, 7.76% of the area was identified as LD and 60.8% of the total area tended to improve, and 31.44% was stable. Most of the regions with LD overlapped with the dryland areas, while improvement areas were identified outside of the drylands. In forested areas from high altitudes, a tendency to improve the condition of vegetation was observed, and most of the surfaces being protected were natural areas that have benefited from proper management. All these results can be used to adapt management practices to avoid, reduce, or restore the LD. The proposed model was based on globally available remote sensing datasets, with a high frequency of data acquisition and collection history that allows for the statistical analyses of changes on a global scale.

**Keywords:** land degradation; desertification; remote sensing; Principal Component Analysis; Romania

## 1. Introduction

Many countries aim to prevent land degradation (LD) and desertification (DS), and promote sustainable land use due to the critical issues they cause, affecting human well-being, biodiversity, and the economy. The most common causes of LD include deforestation [1], agricultural practices, overgrazing [2,3], and climatic changes [4]. To combat land degradation and loss of biodiversity, various policies limit uncontrolled deforestation [5], overgrazing, or the excessive use of fertilizer in agriculture [6]. Extensive areas in southern and south-eastern Europe are affected by the increasing frequency and intensity of droughts [7–9] or heatwave events [10–13]. The Sustainable Development Goal (SDG) 15 aims to “protect, restore and promote sustainable use of terrestrial ecosystems, sustainably manage forests, combat desertification, and halt and reverse land degradation and

halt biodiversity loss" [14]. Recent studies have highlighted an increase in vegetation productivity and a greening trend in natural vegetation, indicating a possible reverse of land degradation [15–17]. Additionally, areas with improved resilience of terrestrial ecosystems to climate change were identified [18].

Different approaches tackle land degradation and desertification at various scales (e.g., global, regional, and national). Globally, the SDG 15.3.1 indicator was developed for LD mapping using three sub-indicators: land cover, land productivity, and soil organic carbon stocks [19]. The World Atlas of Desertification was created using various data, including population dynamics, climate change data, and satellite data related to vegetation productivity [20].

Regionally, the MEDALUS project focused on the Mediterranean area, using indicators related to soil quality, climate factor, the quality of vegetation, and the quality of management [21]. In Romania, land degradation was analyzed through the ecosystem quality outside of protected areas using various types of data, such as land use and land cover data, human settlements, the digital elevation model (DEM), pollution sources, and remote sensing data [22,23].

In this study, the terms LD and DS are defined by the Intergovernmental Panel on Climate Change (IPCC) and UNCCD as follows: LD is a "negative trend in land condition, caused by direct or indirect human-induced processes including anthropogenic climate change, expressed as long-term reduction or loss of at least one of the following: biological productivity, ecological integrity, or value to humans" [20,24,25]; and DS is "land degradation in arid, semi-arid, and dry sub-humid areas resulting from various factors, including climatic variations and human activities" [26–28]. Therefore, desertification is a consequence of the appearance of land degradation in arid, semi-arid, and dry sub-humid areas.

Earth observation data play an essential role in mapping and assessing LD and DS by providing indicators like NDVI, NPP, Evapotranspiration (ET), Land Surface Temperature (LST), and albedo [29–31]. NDVI combined with land use information is frequently used for analyzing LD and DS due to its sensitivity to changes in vegetation cover [32] and is also associated with productivity [33–35]. The negative trend of NDVI denotes an increase in the degree of vegetation wilting in the long term and low productivity. But, recent studies quantified LD based on NPP, which is also useful for global carbon cycle analysis; the decreasing trend of the NPP denotes a decrease in carbon productivity as a result of the reduction in vegetation cover [36–38].

ET is an important indicator for the water cycle, being closely related to soil and plant moisture. It signifies the loss of water due to surface evaporation and transpiration occurring within the vegetation cover. Monitoring ET can help assess water availability and changes in water balance [34]. LST provides critical information about the thermal properties of the land surface. It is frequently used for identifying and monitoring urban heat islands and in the development of green infrastructure [39,40]. A decrease in vegetation cover can lead to higher LST due to reduced transpiration and cooling effects. In non-urban areas, the increase in land surface albedo is often determined by the decrease in vegetation and soil moisture, indicating LD or DS in dryland areas [41,42]. A higher albedo value indicates greater reflectivity, which can result from a decrease in vegetation cover and an increase in bare soil or impervious surfaces [43,44].

The aim of this study is to provide a state-of-the-art approach for assessing the intensity of land degradation and desertification processes using remote-sensing-derived indicators within a GIS environment. The choice of indices such as: NDVI, NPP, albedo, LST, and ET for mapping and LD and DS due to their sensitivity to vegetation changes, capacity to indicate surface properties, and water availability, and their relevance to the study of ecosystems and the Earth's climate system. These indices, when combined with other data sources (meteorological and land cover type) provide valuable insights into the state and dynamics of land degradation and desertification processes.

Principal Component Analysis (PCA) was employed to conduct the analysis, integrating significant trends of relevant biotic and abiotic parameters. Land degradation assessment often involves analyzing a wide range of variables, including soil properties, vegetation indices, and climate data. These datasets can be high-dimensional, making it challenging to identify patterns and relationships. PCA helps by reducing the dimensionality of the data while retaining most of the relevant information. The methodology underwent testing and validation on a national level, but it can be readily applied to other locations, and is contingent upon the accessibility of the required data in a fast and cost-effective manner. Assessing land degradation is essential for decision-makers to effectively manage degraded lands and areas susceptible to desertification. This includes implementing sound agricultural practices, finding drought-resistant plant varieties, promoting soil conservation, and preventing nutrient depletion, especially in arable lands. In the case of forests, it involves sustainable forestry practices, reforestation efforts, and protection against deforestation. For grasslands, it includes responsible grazing management, preventing overgrazing, and implementing measures to combat invasive species that can degrade these ecosystems. These strategies collectively aim to enhance soil quality, maintain biodiversity, and ensure the long-term health and productivity of various land types.

## 2. Materials and Methods

### 2.1. Study Area

This study addresses the national level and covers Romania, a country with an area of approximately 238,400 km<sup>2</sup> situated in south-eastern Europe. According to the Koeppen–Geiger classification [44], there are six types of climates in Romania (Figure 1). The largest area is represented by a humid continental warm summer climate (Dfb) over 147,000 km<sup>2</sup>. The hot summer humid continental climate (Dfa) is the second type of climate that occupies a significant area (approximately 45,000 km<sup>2</sup>). Cold semi-arid climate (BSk) is the third type of climate that occupies a large area in Romania (about 31,000 km<sup>2</sup>).

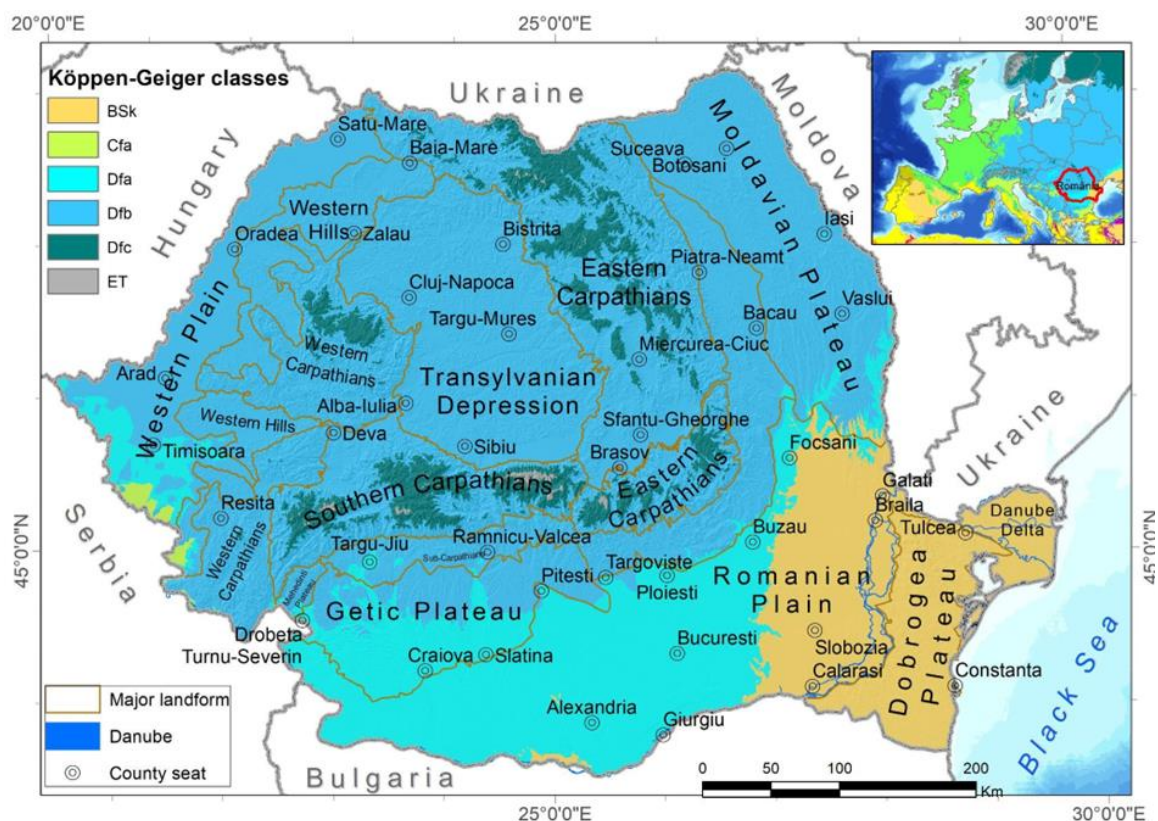


**Figure 1.** Climate types in Romania according to Köppen–Geiger classification (1980–2016) [44] and the geographical location of Romania in Europe (in the medallion).

The main types of land cover and land use in Romania are agricultural land, forest, and grasslands (Figure 2a). Agricultural land occupies large areas in regions with Dfb, Dfa, and BSk climates (Figure 2b), forests and semi-natural areas are found mainly in regions with Dfb and Dfc climates, while the BSk climate includes large areas of wetland ecosystems such as the Danube Delta and the Danube Flood Plain (i.e., Baltile Dunarii, in Romanian).

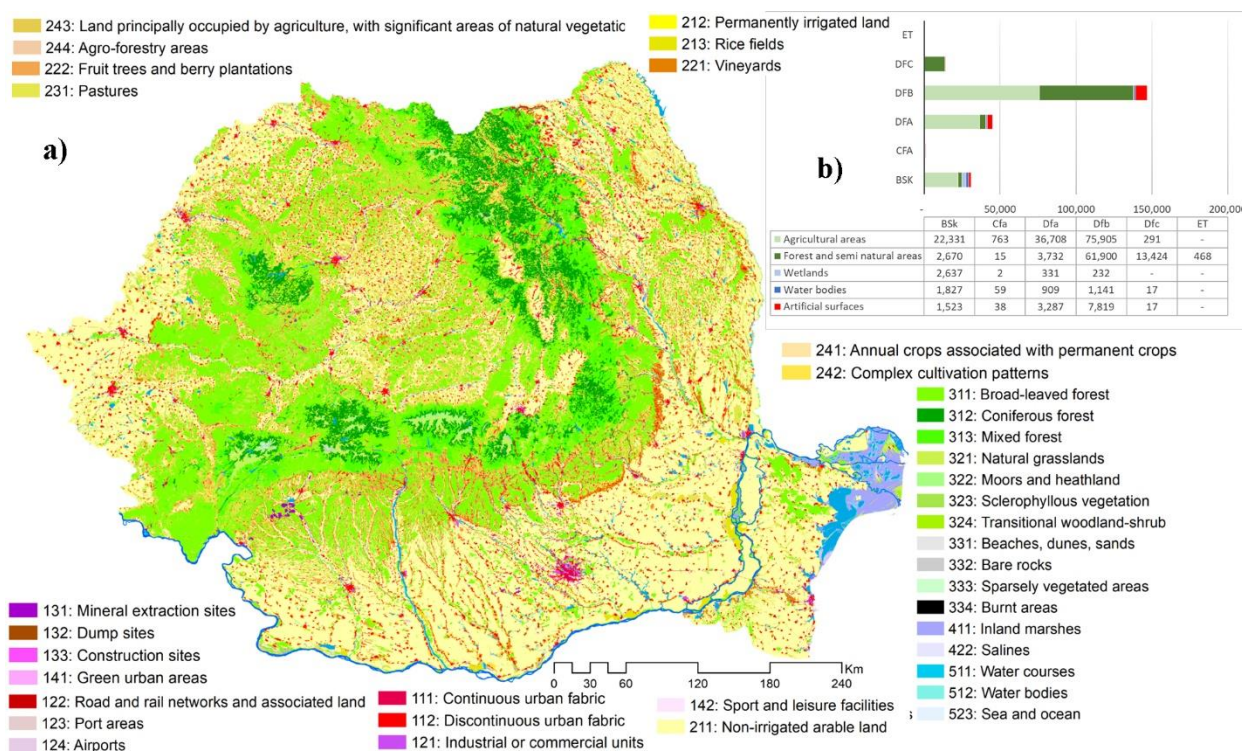


**Figure 2.** (a) Land use in Romania according to Corine Land Cover 2018 [45]. (b) The surface occupied by the main categories of land use in different climatic zones in Romania (in km<sup>2</sup>).

## 2.2. Earth Observation and Auxiliary Data Used for Land Degradation and Desertification Mapping

The changes in vegetation were analyzed over the period 2001–2020 using Moderate Resolution Imaging Spectroradiometer (MODIS) products (Table 1) for the vegetation season (April–September) at a daily temporal resolution [46]. The data were resampled at 500 m spatial resolution and validated with data from the atlas of degraded ecosystems from Romania [22] and Trends.Earth SDG 15.3.1 indicator [19]. Climate data such as precipitation and potential evapotranspiration were used to compute the aridity index used to identify the areas susceptible to desertification. The CORINE Land Cover (CLC) dataset [45] was used to delimit the types of land use as well as other geospatial data such as Koeppen–Geiger climate classification or major landforms.

**Table 1.** Remote sensing and auxiliary data used for LD and DS identification and validation.

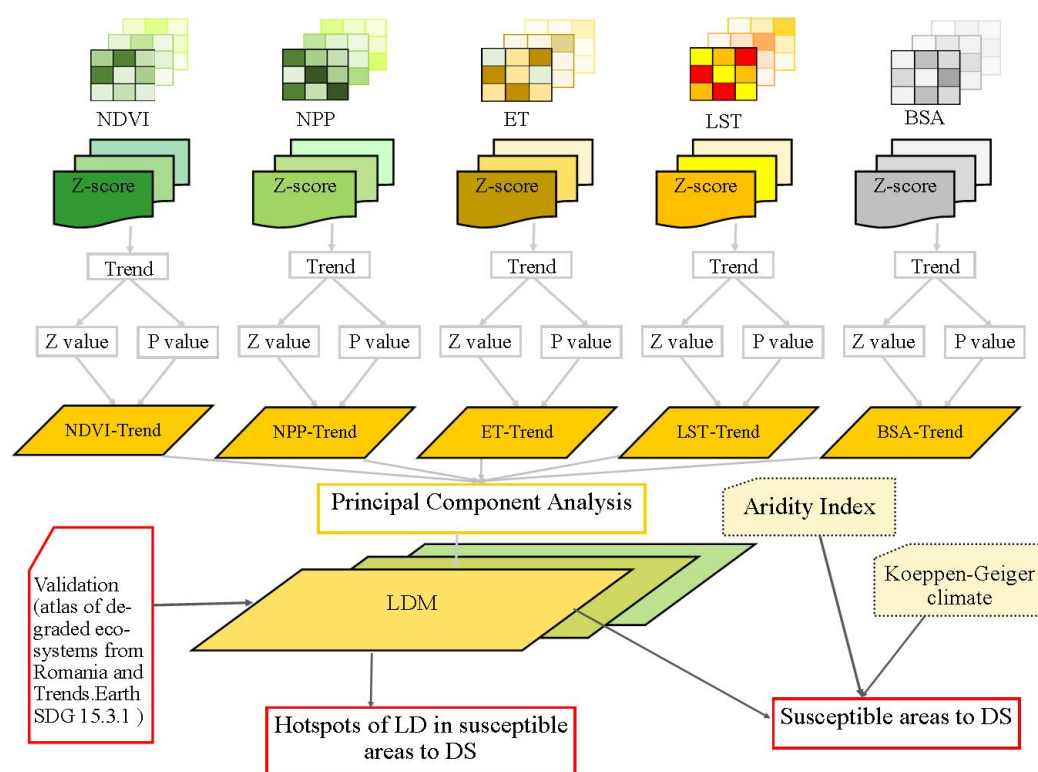
Data Name	Period	Resolution	Data Type	Source
Normalized Difference Vegetation Index (MOD13A1v006)	2001–2020	500 m	raster	NASA EOSDIS [47]
Net photosynthesis (MOD17A2HV6)	2001–2020	500 m	raster	NASA EOSDIS [48]
Total evapotranspiration (MOD16A2v006)	2001–2020	500 m	raster	NASA EOSDIS [49]
Land Surface Temperature (MOD11A2v006)	2001–2020	1000 m	raster	NASA EOSDIS [50]
Black sky albedo (MCD43A3v006)	2001–2020	500 m	raster	NASA EOSDIS [51]
Precipitation (P)	1991–2020	-	vector	National Meteorological Administration
Potential evapotranspiration (ETP)	1991–2020	-	vector	National Meteorological Administration

Table 1. Cont.

Data Name	Period	Resolution	Data Type	Source
CORINE Land Cover (CLC)	2018	100 m	raster	Copernicus Land Monitoring Service [45]
Degraded ecosystems	2016–2018	-	vector	The atlas of degraded ecosystems from Romania [22]
Land degradation indicator	2001–2015	250 m	raster	Trends.Earth SDG 15.3.1 indicator [52]

### 2.3. Methodology

The workflow of this study includes four main stages (Figure 3): 1. the standardization of the MODIS products; 2. the extraction of trends of the relevant variables; 3. the analysis of the principal components (PCs) and computing and validating the LD model; and 4. computing the LD clusters and analyzing the areas within the drylands.



**Figure 3.** Methodological flowchart of this study. NDVI, NPP, ET, LST, and BSA are biophysical parameters; z-score represents the anomaly of each parameter; z value—trend and *p* value—statistical significance according to the Mann-Kendall test; NDVI-Trend, NPP-Trend, ET-Trend, LST-Trend, and BSA-Trend resulted from the combination of the z value and *p* value parameters; LDM—index for assessing the intensity of land degradation.

#### 2.3.1. Z-Score

The average values of the BSA, LST, and NDVI for the vegetation season (April–September) were calculated, as well as the sum of the ET. The NPP represents the sum of the Net photosynthesis index. To remove the scale difference between variables [53], the z-score (anomaly) was extracted as the difference between the biophysical parameters and the multiannual average (for the period 2001–2020), relative to the standard deviation.

#### 2.3.2. Mann-Kendall Test

According to the LD definition [20,25], the trend of the land condition over time is an essential parameter. Therefore, the non-parametric Mann-Kendall test (MK) [54,55] was used for detecting and estimating the trends of the z-score (anomaly of each parameter). The

trend ( $z$  value) was reclassified into two categories (positive values and negative values), and the confidence level ( $p$  value) was reclassified into five classes which were assigned a score from 1 to 5 according to Table 2. This led to five new indicators (NDVI-Trend, NPP-Trend, ET-Trend, BSA-Trend, and LST-Trend) with values between  $-5$  and  $+5$ . Considering that the LD is highlighted by the negative trend of NDVI, NPP, and ET and by the positive trend of LST and BSA, the values of the last two parameters were multiplied by  $-1$  to be consistent with the first three. In the end, all the resulting indicators highlighted the same thing. Thus, positive values between 2 and 5 indicate improved lands, negative values between  $-2$  and  $-5$  indicate degraded lands, and those between  $-1$  and  $+1$  indicate stable lands without significant changes.

**Table 2.** Scores assigned using trend classification ( $z$  value), significance level ( $p$  value), and confidence levels.

Trend (According $z$ Value)	Significance Level ( $p$ Value)	Score *	Confidence Levels
±	0 to 0.001	5	99.9% confidence level
	0.001 to 0.01	4	99% confidence level
	0.01 to 0.05	3	95% confidence level
	0.05 to 0.1	2	90% confidence level
	0.1 to 1	1	<90% No Sig. trend

\* Represents the values assigned to the classes obtained after the classification.

### 2.3.3. Principal Component Analysis

In this study, the Principal Component Analysis (PCA) method [56] was employed to aggregate the five resulting indicators (NDVI-Trend, NPP-Trend, ET-Trend, BSA-Trend, and LST-Trend) which were described in Section 2.3.2. PCA is commonly used to reduce the number of variables by identifying the principal components. It transforms the original variables into a smaller number of uncorrelated datasets (principal components) that capture the most significant variations in the data. This simplification makes it easier to detect patterns associated with land degradation. Each principal component is associated with eigenvectors; these eigenvectors can be used to obtain the weights for LD indices.

The five main components were obtained based on the five variables used as input in the principal components (Spatial Analyst) tool from ArcGIS toolbox [57]. The PCA tool generated new raster datasets where each raster represents a principal component. Each principal component is a linear combination of the original datasets, and they highlight different features or information in the data (Figure S1). Also, each PC is represented by a set of eigenvectors, which are the proportion with which each variable contributes to obtaining PC1, PC2, PC3, etc. [53]. These values can range between  $\pm 1$  and 0. The closer they are to  $\pm 1$ , the greater the contribution of the analyzed variables, while values closer to 0 indicate a smaller contribution. The sign (positive or negative) shows the direction that a given variable in that PC is going on a single dimension vector.

The results from the PCA revealed that PC1 alone explains 61.24% of the variance, followed by PC2 with 14.57%, PC3 with 9.82%, PC4 with 7.83%, and PC5 with 6.53%. The cumulative eigenvalues demonstrated that the first four components collectively account for 93.47% of the variance (Table 3 and Figure S2 in Supplementary Material). As a result, the first four PCs were used to compute the Land Degradation Model (LDM).

**Table 3.** Principal Component Analysis.

PC	PC1	PC2	PC3	PC4	PC5	
Eigenvectors	NDVI-Trend	0.60243	0.17929	0.55936	0.53391	0.08364
	NPP-Trend	0.00131	0.61281	0.40223	-0.57068	-0.37014
	ET-Trend	0.19080	0.70214	-0.60794	0.14125	0.28471
	BSA-Trend	0.77391	-0.31466	-0.27073	-0.47023	-0.08743
	LST-Trend	0.04174	0.01780	-0.28714	0.38497	-0.87595
Eigenvalues	5.30789	1.26291	0.85149	0.67895	0.56581	
Percent of Eigenvalues (%)	61.2422	14.5714	9.8244	7.8337	6.5283	
Accumulative of Eigenvalues (%)	61.2422	75.8136	85.6381	93.4717	100	

In this study, in the structure of PC1, BSA-Trend contributed the most, followed by NDVI-Trend, while NPP-Trend contributed the least. Therefore, a significant proportion of the information related to the degradation phenomenon can be obtained through the analysis of these two variables alone. However, there remains an approximately 40% portion that cannot be explained by PC1. In this regard, it is necessary to calculate PC2, where ET-Trend and NPP-Trend significantly contribute. In other words, these are the next two variables that complement the information captured by PC1, adding an approximately 14% contribution. ET-Trend and NDVI-Trend significantly contribute to the calculation of PC3, explaining approximately 9.8% of the information related to degraded lands, while PC4 is highlighted through the use of the variables NDVI-Trend, BSA-Trend, and NPP-Trend. It can be observed (Table 3) that LST-Trend has the smallest contribution in the first four PCs but a significant contribution to PC5. However, PC5 explains only 6.5% of the phenomenon, while the first four PCs combined explain over 90% of the phenomenon. Therefore, we can rely on the analysis of the first four components for identifying degraded lands.

Finally, the five PCs were aggregated into a single LD model using a linear Equation (1). To achieve this, the value of the percent of eigenvalues was divided by 100 for each PC to scale values from 1–100 to 0–1. The obtained values were classified into three equal intervals representing land degradation, stable land, and improvement (Table 4).

$$\text{LDM} = 0.612422 \times \text{PC1} + 0.145714 \times \text{PC2} + 0.098244 \times \text{PC3} + 0.078337 \times \text{PC4} \quad (1)$$

**Table 4.** LDM value classification.

Values	Description
<−1	Land Degradation
−1 to 1	Stable
>1	Improvement

#### 2.3.4. Evaluation of the LDM Performance

The receiver operating characteristics (ROC) analysis was used to evaluate the LDM performance. Several statistical indices like sensitivity, specificity, accuracy, and Area Under the Curve (AUC) were calculated [58]. The ROC curve is a method that compares true positive rates against false positive rates. The ROC analysis was performed using the roc() function implemented in the pROC R package [59].

The results of the model were compared with the forest ecosystem and grassland ecosystem evaluations from the atlas of degraded ecosystems from Romania [22] and with the LD data from Trends.Earth SDG 15.3.1 [52]. It has to be mentioned that the atlas of degraded ecosystems in Romania contains information about the degradation of grassland and forest ecosystems; it does not include an assessment of arable land or other types of land cover or use. Therefore, the information from Trends.Earth SDG 15.3.1 was used to validate degraded arable land and other types of land use or cover. From what is known so far, in Romania there are no other data related to land degradation that can be used for validation. Therefore, 400 points were randomly chosen for forest ecosystems (from the atlas of degraded ecosystems from Romania), 600 for grassland ecosystems (also from the atlas of degraded ecosystems), 900 for arable land (from Trends.Earth SDG 15.3.1), and 2500 points for all types of land use to cover all the counties of Romania (from Trends.Earth SDG 15.3.1).

Generally, a value of AUC greater than 70% indicates relatively good prediction [60] (Table 5). In this study, the AUC for forest ecosystems was 81.2%, for grassland ecosystems 84.5%, 77.9% for arable land, and for all types of land use AUC was 71.8%, in general showing satisfactory results (Figure 4). The highest values are in the case of forest and grassland ecosystems, with the results being compared with data from the atlas of degraded ecosystems from Romania. The lowest were in the case of arable land and other types of

use, with the results being compared with data from Trend.Earth SDG 15.3.1. The difference between the validation results may be due to the data sources used for validation.

**Table 5.** Interpretation of the Area Under the Curve [60].

Area Under the Curve (AUC)	Interpretation
$90\% \leq \text{AUC}$	Excellent
$80\% \leq \text{AUC} < 90\%$	Good
$70\% \leq \text{AUC} < 80\%$	Fair
$60\% \leq \text{AUC} < 70\%$	Poor
$50\% \leq \text{AUC} < 60\%$	Fail

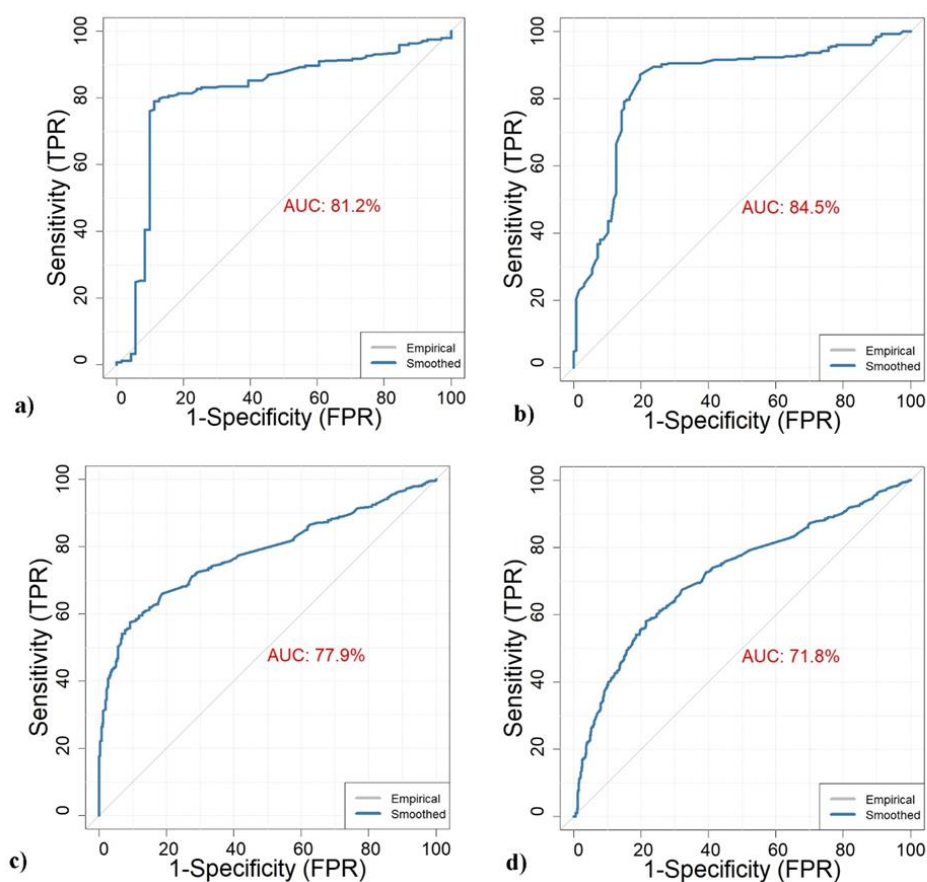


**Figure 4.** The ROC and AUC for (a) forest ecosystems, (b) grassland ecosystems, (c) arable land, and (d) for all other type of land use (including agriculture and natural areas).

### 2.3.5. The Degree of Climate Susceptibility to Desertification Processes

The degree of climate susceptibility to desertification processes was highlighted by the intersection of two thematic layers, the Koeppen-Geiger climate types (Bsk, Cfa, and Cfb) and the dryland areas (aridity index between 0.2 and 0.65) determined for the period 1991–2020. Climate types like Bsk, Cfa, and Cfb are associated with different levels of temperatures and precipitation patterns. Areas with arid or semi-arid climates (such as Bsk) are more susceptible to desertification due to their limited water availability, while areas with humid climates (such as Cfa and Cfb) are generally less susceptible. The dryland (arid, semi-arid, and dry sub-humid areas) represents all areas in which the ratio between precipitation (P) and evapotranspiration (PET) has values between 0.05 and 0.65 [28,61]. The ratio is known as the UNEP Aridity Index (AI), which is frequently used in studies on a national [7,62] and global scale [63]. Areas with lower aridity index values have lower water availability, which can make them more prone to desertification processes [64]. The

specified range of aridity index values (0.05 to 0.65) likely represents a critical threshold where the risk of desertification increases significantly [65].

By integrating both climate types and aridity index values, a more comprehensive assessment of desertification sensitivity was created. Regions that fall into the specified climate types and also have aridity index values within the defined range are likely to face a higher risk of desertification. This combined approach considers both the long-term climatic conditions and the immediate aridity levels, providing a more nuanced understanding of desertification vulnerability. Four classes were created in which values are assigned from  $-1$  (slightly susceptible areas) to  $-4$  (extremely susceptible areas) (Table 6). In Romania, only the semi-arid and dry sub-humid classes (between 0.2 and 0.65) were identified for the period 1991–2020. To identify areas with DS processes, the LD values lower than  $-1$  from LDM (Table 4) are intersected with the four classes of degrees of climate susceptibility to desertification (Table 6).

**Table 6.** The degree of climate susceptibility to desertification processes.

Dryland Areas (Aridity Index between 0.2 and 0.65)	Koepfen-Geiger Climate Types	Degree of Climate Susceptibility to DS	Score
Semi-arid	BSK	Extremely susceptible areas (ESA)	$-4$
	Cfa	High susceptible areas (HSA)	$-3$
Dry sub-humid	Cfa	Moderately susceptible areas (MSA)	$-2$
	Cfb	Slightly susceptible areas (SSA)	$-1$

### 2.3.6. Land Degradation and Desertification Hot Spots

To identify the statistical significance of DS process hot spots, the Getis-Ord  $G_i^*$  method [66] was applied. This method is computed based on standard normal distribution. The Hot Spot Analysis was performed in ArcGIS using the Mapping Clusters toolset [67]. The statistical significance is based on the z-score (Standard Deviations) and P-value (Probability) and it was calculated for 90%, 95%, and 99% confidence levels (Table 7). The clusters were created based on the mean values of DS within the 10 km resolution cell grid.

**Table 7.** The statistical significance of hot and cold spots according to Getis-Ord  $G_i^*$  statistics.

z-Score (Standard Deviations)	p-Value (Probability)	Confidence Level
$<-1.65$ or $>+1.65$	$<0.10$	90%
$<-1.96$ or $>+1.96$	$<0.05$	95%
$<-2.58$ or $>+2.58$	$<0.01$	99%
$-1.65$ to $+1.65$	$>0.10$	$<90\%$ Not statistically significant

## 3. Results

### 3.1. Trend of Remote Sensing Indices in Romania

To provide an overview of the BSA-Trend, LST-Trend, NDVI-Trend, NPP-Trend, and ET-Trend spatial distribution, the values were divided into four classes (decreasing between 0 and  $-1$ , significantly decreasing below  $-1$ , increasing between 0 and 1, and significantly increasing above 1) and the surface of each category relative to the total per country was calculated. Also, the evaluation of the spatial distribution was completed at the local level (by major landforms and main land cover). The spatial distribution of the increasing trends (increasing and significantly increasing) of BSA-Trend, LST-Trend, NDVI-Trend, NPP-Trend, and ET-Trend are presented in Figure 5.

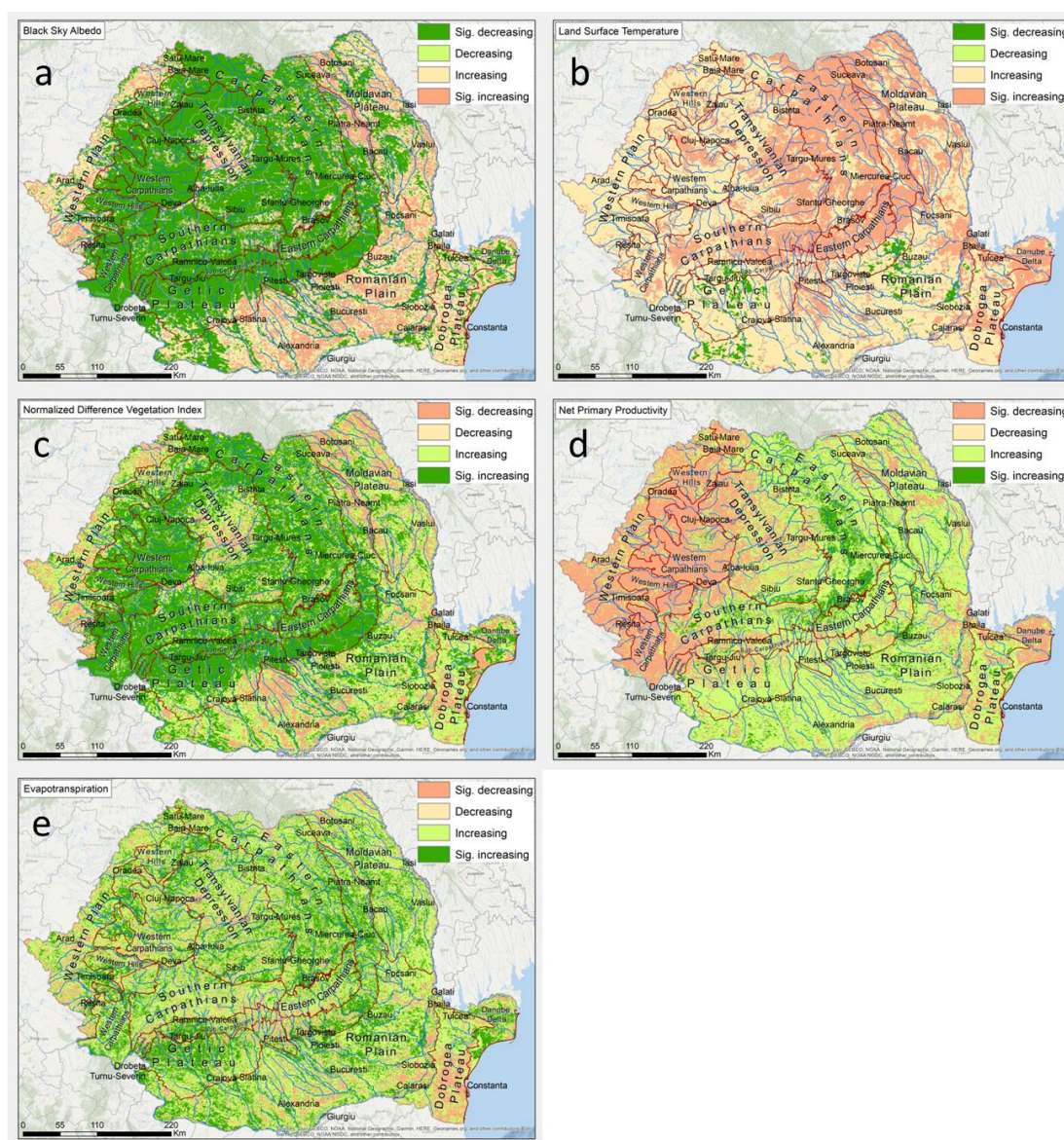


**Figure 5.** Spatial distribution of remote sensing index trends: (a) Black Sky Albedo; (b) Land Surface Temperature; (c) Normalized Difference Vegetation Index; (d) Net Primary Productivity; (e) Evapotranspiration.

### 3.1.1. Black Sky Albedo

Extensive areas with increasing trends were noted in the south-eastern part of Romania (in the Dobrogea Plateau, the Danube Delta, and in the Romanian Plain), the north-east (in the Moldavian Plateau), the west (in the Western Plain), and partially in the central part (Depression of Transylvania) (Figure 5a).

In total, 12.14% of Romania's surface had BSA with significantly increasing trends and 31.75% with significantly decreasing trends. The decreasing trend of BSA was observed especially in the mountainous areas (the total was 29.21% of which 18.35% was significantly decreasing trends) while the increase was registered in the lower areas of Romania (the total was 21.48% of which 6.75% was significantly increasing trends). The percentage distribution of BSA trend classes in major landforms compared to the total surface of Romania are presented in the Supplementary Material (Figure S3).

Arable land occupied 36.32% of the country's surface, of which 25.86% was increasing (17.14% increasing and 8.71% significantly increasing) and 10.46% decreasing (7.18%

decreasing and 3.28% significantly decreasing). The forest surface occupied 29.9% of the country's surface of which only 4.58% was increasing (3.67% increasing and 0.9% significantly increasing). The percentage distribution of trend classes in main land cover compared to the total surface of Romania are presented in the Supplementary Material (Figure S4).

### 3.1.2. Land Surface Temperature

Most of Romania's surface is warming, but from among all the regions of the country, significantly increasing trends were observed in the central-eastern part (the Eastern and the Southern Carpathians) (Figure 5b). The largest surfaces with increasing trends of LST were observed in the hill and plateau areas (the total was 35.3% of which 11.96% was significantly increasing trends) and in mountainous areas (the total was 34.22% of which 18.14% was significantly increasing trends) (Figure S3 in the Supplementary Material). Most of the significantly increasing trends took place in forest areas (14.94%) and arable land (8.33%) (Figure S4 in the Supplementary Material).

### 3.1.3. Normalized Difference Vegetation Index

According to the results, only a few areas in Romania had decreasing trends of NDVI (15.1%, of which 7.17% was in plain areas). Significantly decreasing trends were registered on only 0.78% of plain areas, 0.54% of hills and plateaus, and 0.21% of mountains (Figure S3). Significant decreases were noticed in 0.84% of the arable land areas, 0.1% of the grassland areas, and 0.09% of the forest areas (Figure S4). The increases were observed especially in the mountainous areas (33.14%, of which 26.52% was significantly increasing trends), while the decreases were reported in the lower areas of Romania such as the Western Plain, Romanian Plain, and Danube Delta, and also in the center of the Dobrogea Plateau (Figure 5c).

### 3.1.4. Net Primary Productivity

The trends of NPP indicated large areas of decrease in the western part of Romania, but they were statistically insignificant in most landforms (in the Western Plain, the Crisana Hills, and the Western Carpathians) (Figure 5d). In total, 33.56% of Romania's surface had decreasing trends of NPP, of which 1.61% was significantly decreasing (0.61% in mountain areas, 0.55% in hills and plateaus, and 0.43 in plain areas). From a land cover point of view, 13.5% of forest areas, 9.6% of the arable land, and 4.87% registered a decreasing trend (of which only 0.67%, 0.44%, and 0.24%, respectively, were significantly decreasing) (Figure S4).

### 3.1.5. Evapotranspiration

Small areas in Romania registered a decreasing trend of ET (the total was 14.62%, of which only 0.64% was significantly decreasing). This was observed mostly in the south-eastern part of the country (Dobrogea Plateau) (Figure 5e). This was known for its arid nature, and the decreasing trend of ET accentuates this condition. The most affected were the arable lands, where 6.21% had a decreasing trend, of which 0.33% was significant.

## 3.2. Land Degradation and Desertification Assessment

According to the LDM, a small percentage (7.76% of the total area of Romania) was identified as degraded lands. Most of the degraded surfaces were in areas with arable land (15% of the total area of arable land in Romania), followed by grassland (5.2% of the total area of grassland), and forests (1.2% of the total area of forests). LD areas were located predominantly in the center of the Dobrogea Plateau, followed by southeast of the Romanian Plain, the south of the Western Plain, the north of the Moldavian Plateau, and the Sub-Carpathians, as well as the center of the Transylvanian Depression (Figure 6). Meanwhile, extensive areas in Romania tended to improve between 2001 and 2020 (60.8% of the total area), especially in the Carpathian and Sub-Carpathian areas, and 31.44% of the

total area was stable. Most of these areas have been declared protected areas and many of them have a management plan to conserve biodiversity.

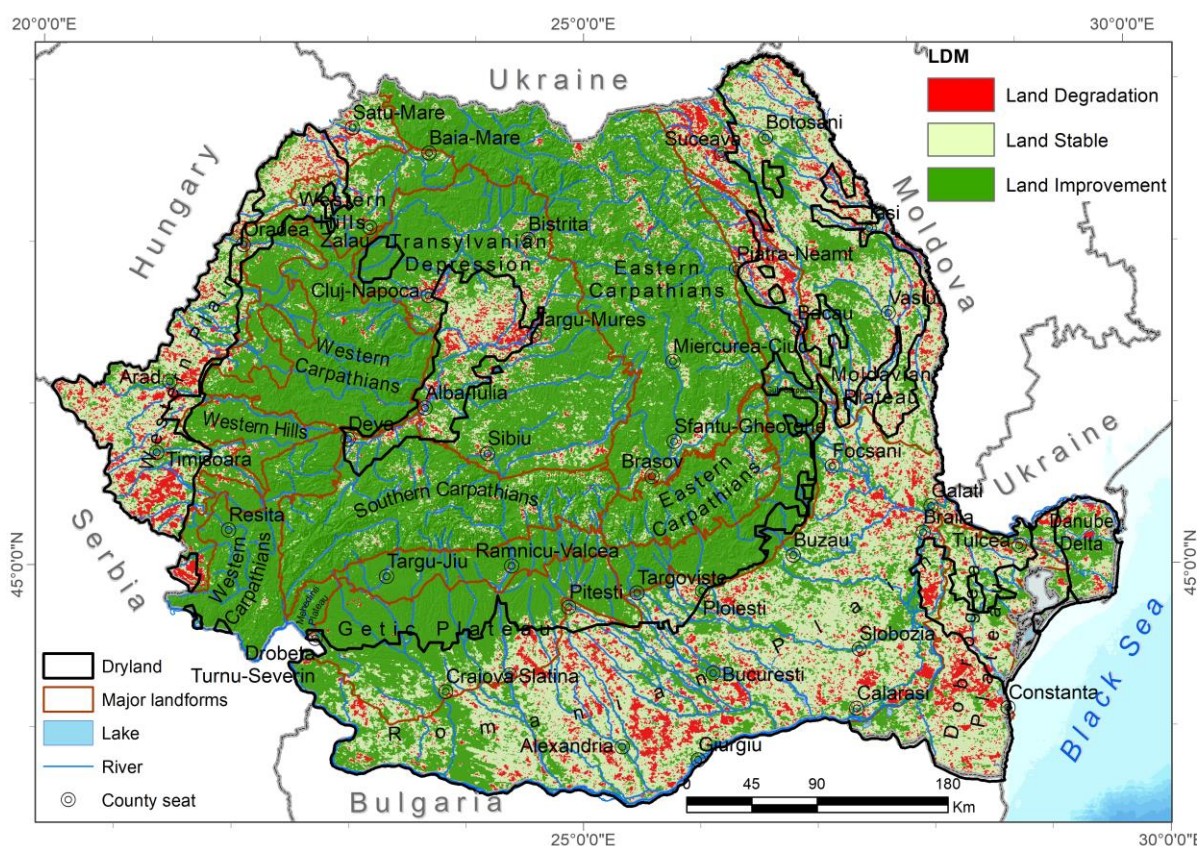


**Figure 6.** Spatial distribution of land degradation in Romania.

According to the LDM, the largest area of degraded arable land was in the Romanian Plain of 5092.8 km<sup>2</sup> (14.79% of its arable land) followed by the Western Plain with 2458.86 km<sup>2</sup> (21.23% of the arable land), the Moldavian Plateau with 2080.56 km<sup>2</sup> (18.37% of the arable land), and the Dobrogea Plateau with 1072.53 km<sup>2</sup> (15.95% of the arable land). Table S1 shows the percentage values at the level of major landforms and main types of land use and Table S2 shows the absolute values in km<sup>2</sup> with land degradation (LD), stable lands (S), and total improvement surfaces (I). The largest degraded forest area was identified in the eastern Carpathians of 187.3 km<sup>2</sup> (which represents 1.14% of the total forest area in this area), followed by the Romanian Plain with 127.84 km<sup>2</sup> (4.34% of the total forest area), the Moldavian Plateau with 115.3 km<sup>2</sup> (3.37% of the total forest area), the southern Carpathians with 83.38 km<sup>2</sup> (0.88% of the total forest area), and the Transylvanian Depression with 49.68 km<sup>2</sup> (0.85% of the total forest area). The largest surface extension of the degraded grassland was present in the Moldavian Plateau, 395.19 km<sup>2</sup> (12.67% of the total grassland area), followed by the Transylvanian Depression, 353.62 km<sup>2</sup> (5.42% of the total grassland area), and the Western Plain, 331.58 km<sup>2</sup> (17.61% of the total grassland area).

By aggregating the dryland areas (according to the AI values) with the LD in Romania, it turned out that the largest areas affected by desertification process were in the central part of the Dobrogea Plateau, the center and east of the Romanian Plain, and the south of the Western Plain (Figure 7). In the Dobrogea Plateau, approximately 1236 km<sup>2</sup> of land was exposed to DS, of which 1072.55 km<sup>2</sup> was arable lands and 147.65 km<sup>2</sup> was grasslands. In the Romanian Plain, 5253.87 km<sup>2</sup> was exposed to desertification, and in the Western Plain, 2431.92 km<sup>2</sup>.

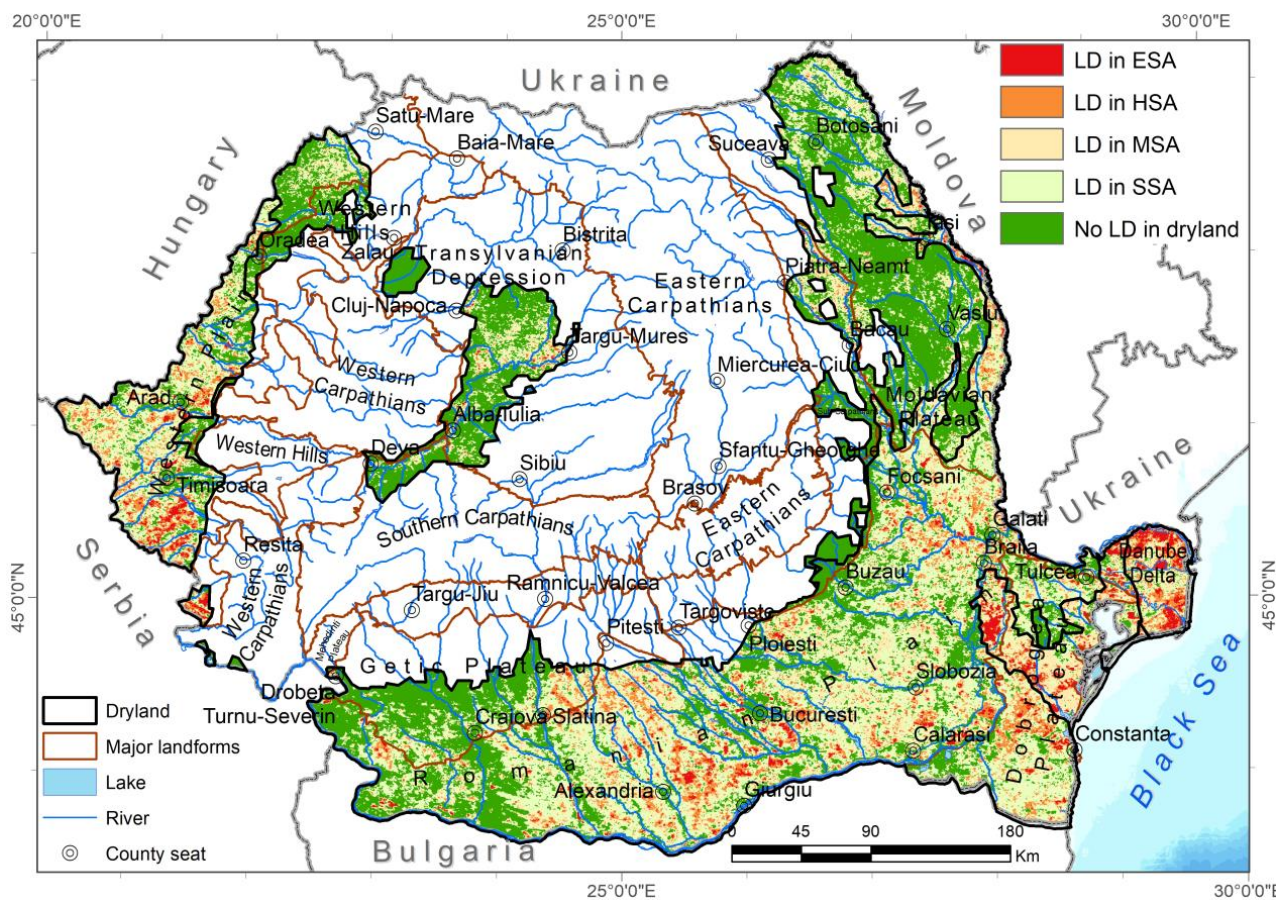


**Figure 7.** Spatial distribution of LD in susceptible areas to DS processes in Romania. ESA represents extremely susceptible areas, HSA—high susceptible areas, MSA—moderately susceptible areas, and SSA—slightly susceptible areas.

### 3.3. Hot Spots of Land Degradation in Areas Susceptible to Desertification

Clustering provided an overview of areas with high concentrations of LD, and stable or improvement surfaces in areas susceptible to DS. The clusters obtained based on the Getis-Ord  $G_i^*$  method highlighted hot spots with 99% confidence of the degraded lands in the Dobrogea Plateau, extensive areas of the Romanian Plain, the Western Plain, the Moldavian Plateau and the center of the Transylvanian Depression (Figure 8). These mostly overlap with the dryland areas, which means that they were susceptible to desertification. In these areas, management measures need to be applied to improve the quality of the land. On the other hand, extensive areas of the mountain and plateau areas (except for the Moldavian Plateau and the center of the Transylvanian Depression) recorded cold spots with 99% confidence.

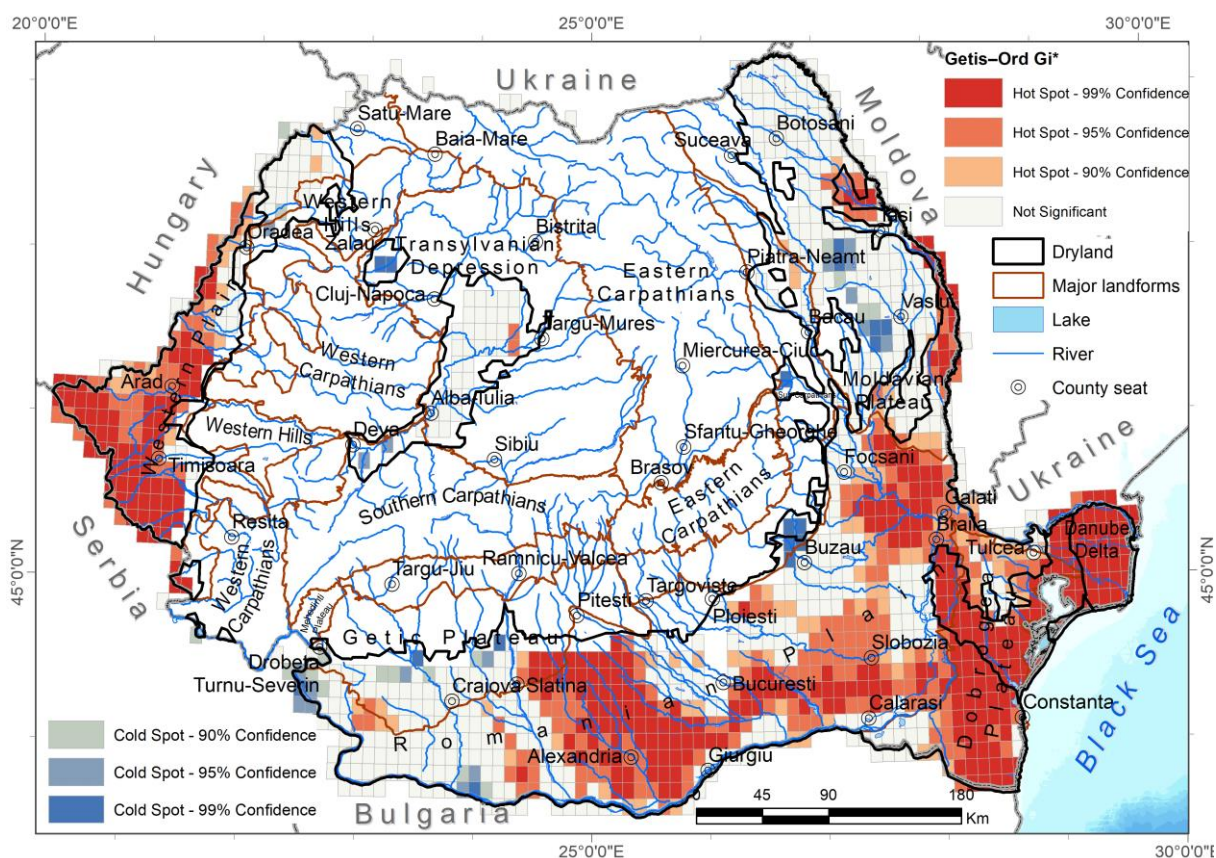


**Figure 8.** Hot spots of LD in areas susceptible to DS processes. Confidence levels indicate the thresholds for which the null hypothesis is rejected.

#### 4. Discussion

The EO data were frequently used for the identification of land degradation on an international scale. Some studies use land surface albedo, others vegetation indices such as NDVI or NPP [25]. UNCCD recommends land cover, land productivity, and soil organic carbon stocks [19]. A summary of the LD obtained based on the Trends.Earth SDG 15.3.1 indicator [19] at the level of Romania for the period 2000–2015 indicates 9.89% of the land area degraded from the total land area, 66.41% improved land area, and 23.33% stable land area. The values were very close to those obtained in this study (7.76% of the total area of Romania was LD, 60.8% of the total area tended to improve, and 31.44% was stable), in which the PCA was used to aggregate remote sensing indices into a single LDM. It is very likely that the differences between the results were due to the length of the analysis period (2000–2015 for Trends.Earth SDG 15.3.1 indicator versus 2001–2020 for our model).

In previous studies, various areas that were susceptible to degradation and desertification were identified, most of them due to climate changes that cause frequent dry events such as those in the Dobrogea Plateau and the eastern Romanian Plain [68,69], and in other areas due to soil erosion and landslides such as those in the Moldavian Plateau [70,71] and some areas in the Transylvanian Depression [72,73]. Also, soil erosion was identified in various areas of the Dobrogea Plateau [74], a phenomenon potentiated by overgrazing [75,76]. The results of our study confirm the occurrence of land degradation in all these areas, but the spatial extension according to our results was less extended than previously estimated.

Cheval (2020) found a high intensity of climate change hot spots determined especially by air temperatures in the north-western part of Romania (Western Plain, Crisana Hills, Western Carpathians, and Transylvanian Depression), in the central-southern part (southern Carpathians and Getic Plateau), and also in the eastern part of the country (the Dobrogea Plateau and the southern half of the Moldavian Plateau) [77]. However, the vegetation

responds differently to these climate changes depending on its level of species resilience and adaptation, thereby explaining the increasing trends of the forest vegetation in the mountain area. Arable land, on the other hand, was more affected by these climate changes compared to land covered by natural vegetation (forest and grassland).

The sandy area in the west of the Romanian Plain, called “Sahara of Oltenia” by Romanians, was considered to be susceptible to desertification because of the destruction of the irrigation system in the post-communist period, the deforestation of forests, and forest protection belts [78–81]. All this led many farmers to give up agricultural activities, and much agricultural land was abandoned. There were studies that have shown that a greening of vegetation can be observed on abandoned agricultural lands [82]. Also, in some areas, the increase in tree cover was caused by the abandonment of farms even in critical regions such as the savannah of Africa [83]. According to our model, there were land improvements in this part of the country, and the extended surface was covered by vegetation (a greening of vegetation). The agricultural crops were replaced by natural steppe vegetation. Moreover, this area is currently a Special Protection Area (SPA) [84,85]. This is proof of the resilience of species and habitats despite climate change. Without human intervention, nature restores itself. However, a balance between the need to preserve biodiversity and the need to feed people is required. Not all of Romania’s agricultural surfaces must be returned to nature, replaced by natural vegetation, but neither should they be replaced by agricultural land. Therefore, it is recommended to practice sustainable, environmentally friendly agriculture [86].

The spatial distribution of the LD suggests that most degraded arable lands were intensively exploited by farmers. A high share of LD processes can also be observed around big cities (Figure 6) such as Bucharest-Alexandria, Constanta, Cluj-Napoca, Targu Mures, and Timisoara, etc. The increasing demand of food products in urban concentrations, in many cases, determined the farmers’ increase in production, to the detriment of the land quality [87]. It was proven that intensive agriculture without an adequate rotation of crops, and the use of various chemical fertilizers in quantities exceeding the accepted limit, can cause land degradation [86]. Also, the building demand determined the expansion of the cities towards the suburbs, with much agricultural land being replaced by built-up areas [87]. Moreover, people’s demand for accessibility and the development of the road network determined the replacement of agricultural or forest land with impervious areas; for example, the highway between the cities Deva, Alba-Iulia, and Cluj-Napoca, in the central part of the country, where the impact on the surrounding area can be clearly seen (Figure S5 in the Supplementary Material). All this leads to the degradation of the lands near the built-up areas by increasing the concentrations of pollutants and deforestation, increasing the temperature, and the fragmentation of habitats [87], all with an impact on the quality of life of the population as well as biodiversity.

This study was carried out based on satellite images, and the results have some inherent limitations. For example, the spatial resolution of the images (500 m), does not allow for the identification of smaller degraded surfaces. Also, crop rotation for arable land could induce errors in the analysis of trends; therefore, the recommendation is an analysis of the types of crops each year for a better accuracy of the model in these areas. However, acknowledging the degree of error of the model, the results can be extremely useful in the identification and monitoring of degraded lands on extensive surfaces, saving part of the financial resources and time spent in the field collecting data.

## 5. Conclusions

This study provides a state-of-the-art approach to assess the intensity of land degradation and desertification processes, with PCA demonstrating its suitability for this purpose. To identify degraded lands, the first step is to compute long-term trends of relevant biophysical parameters, such as NDVI, NPP, BSA, ET, and LST; then, the trends of remote sensing products between 2001 and 2020 are integrated to achieve optimal results, considering the climate change perspective. This methodology uses satellite images with a high frequency

of data acquisition and collection history that allows for the statistical analyses of changes on a global scale.

Also, the results of the study are based on the first four principal components (PCs). PC1 is primarily composed of the variables NDVI-Trend and BSA-Trend, contributing to the final analysis with a weight of 61.24%. PC2 is composed of ET-Trend and NPP-Trend and contributes 14.57%. PC3 is composed of ET-Trend, NDVI-Trend, and NPP-Trend, contributing 9.82%. PC4 is composed of NPP-Trend, NDVI-Trend, and BSA-Trend, contributing 7.8%.

PCA not only helps reduce the number of indicators but also identifies the most significant ones. Moreover, the results obtained by the weighted aggregation of all the identified components are superior to those obtained by individually analyzing each indicator. The results obtained using PCA are consistent with those obtained in previous studies over a shorter period (2016–2018) and validated in the field at the national level, as well as with those conducted globally over a longer period (2001–2015) but not validated in Romania.

Our findings reveal that LD processes cover 7.76% of Romania's total area, while the category of 'no land degradation' prevails, representing 60.8% of the total area with an improvement trend and 31.44% remaining stable. The hot spots of LD exposed to DS were predominantly observed in the south-eastern part of Romania (the Dobrogea Plateau and the Romanian Plain), the Western Plain, and the Moldavian Plateau.

These findings bear significant importance for decision makers in effectively managing degraded lands and those prone to DS processes. By adopting suitable agricultural practices and selecting drought-resistant plant varieties that enrich the soil without depleting nutrients, we can strive to improve soil quality and combat desertification, paving the way towards sustainable land use management.

**Supplementary Materials:** The following supporting information can be downloaded at: <https://www.mdpi.com/article/10.3390/rs15194842/s1>, Figure S1: The spatial distribution of the values of the principal components; Figure S2: The percentage of the accumulation of eigenvalues captured by the principal components; Figure S3: The percentage of the distribution of trend classes in major landforms compared to the total surface of Romania; Figure S4: The percentage of the distribution of trend classes in main land cover compared to the total surface of Romania; Figure S5: Spatial distribution of land degradation in the Deva, Alba-Iulia, Cluj-Napoca, and Targu-Mures areas; Table S1: Total surfaces (%) with land degradation (LD), stable lands (S), and total improvement surfaces (I) at the level of major landforms and main types of land use; Table S2: Total surfaces (km<sup>2</sup>) with land degradation (LD), stable lands (S), and total improvement surfaces (I) at the level of major landforms and main types of land use.

**Author Contributions:** Conceptualization, I.O. and S.C.; Formal analysis, G.B.; Methodology, I.O. and S.C.; Resources, A.I.; Software, I.O. and V.-A.A.; Supervision, A.I.; Validation, I.O.; Visualization, I.O. and G.B.; Writing—original draft, I.O.; Writing—review and editing, S.C., A.I., G.B., V.-A.A., D.M., A.N., C.-V.A. and V.C. All authors have read and agreed to the published version of the manuscript.

**Funding:** This research was partially funded by the Romanian National Meteorological Administration.

**Acknowledgments:** The authors acknowledge three anonymous reviewers for their useful comments on the paper. We acknowledge the meteorological database department who provided observations from the national meteorological network.

**Conflicts of Interest:** The authors declare no conflict of interest. The funders had no role in the design of the study; in the collection, analyses, or interpretation of data; in the writing of the manuscript; or in the decision to publish the results.

## References

1. Dimobe, K.; Ouédraogo, A.; Soma, S.; Goetze, D.; Porembski, S.; Thiombiano, A. Identification of Driving Factors of Land Degradation and Deforestation in the Wildlife Reserve of Bontioli (Burkina Faso, West Africa). *Glob. Ecol. Conserv.* **2015**, *4*, 559–571. [CrossRef]
2. Angerer, J.P.; Fox, W.E.; Wolfe, J.E. Chapter 11.3—Land Degradation in Rangeland Ecosystems. In *Biological and Environmental Hazards, Risks, and Disasters*; Shroder, J., Sivanpillai, R., Eds.; Academic Press: Boston, MA, USA, 2016; pp. 277–311. ISBN 978-0-12-394847-2.
3. Bhunia, G.S.; Chatterjee, U.; Shit, P.K.; Kashyap, A. Chapter 5—Wasteland Reclamation and Geospatial Solution: Existing Scenario and Future Strategy. In *Land Reclamation and Restoration Strategies for Sustainable Development*; Academic Press: Cambridge, MA, USA, 2021; Volume 10, pp. 87–113. ISBN 1363-0814.
4. Shukla, P.R.; Skea, J.; Buendia Calvo, E.; Masson-Delmotte, V.; Pörtner, H.-O.; Roberts, D.C.; Zhai, P.; Slade, R.; Connors, S.; Diemen, R.; et al. (Eds.) IPCC Summary for Policymakers. In *Climate Change and Land: An IPCC Special Report on Climate Change, Desertification, Land Degradation, Sustainable Land Management, Food Security, and Greenhouse Gas Fluxes in Terrestrial Ecosystems*; Intergovernmental Panel on Climate Change (IPCC): Geneva, Switzerland, 2019.
5. European Commission. EU Forest Policies. Available online: <https://ec.europa.eu/environment/forests/fpolicies.htm> (accessed on 5 December 2022).
6. European Commission. EU Soil Policy. Available online: [https://ec.europa.eu/environment/soil/soil\\_policy\\_en.htm](https://ec.europa.eu/environment/soil/soil_policy_en.htm) (accessed on 5 December 2022).
7. Cheval, S.; Dumitrescu, A.; Birsan, M.-V. Variability of the Aridity in the South-Eastern Europe over 1961–2050. *CATENA* **2017**, *151*, 74–86. [CrossRef]
8. Jaagus, J.; Aasa, A.; Aniskevich, S.; Boincean, B.; Bojariu, R.; Briede, A.; Danilovich, I.; Castro, F.D.; Dumitrescu, A.; Labuda, M.; et al. Long-Term Changes in Drought Indices in Eastern and Central Europe. *Int. J. Climatol.* **2022**, *42*, 225–249. [CrossRef]
9. Spinoni, J.; Naumann, G.; Vogt, J.V. Pan-European Seasonal Trends and Recent Changes of Drought Frequency and Severity. *Glob. Planet. Chang.* **2017**, *148*, 113–130. [CrossRef]
10. Croitoru, A.-E.; Piticar, A.; Ciupertea, A.-F.; Roșca, C.F. Changes in Heat Waves Indices in Romania over the Period 1961–2015. *Glob. Planet. Chang.* **2016**, *146*, 109–121. [CrossRef]
11. Nagavciuc, V.; Scholz, P.; Ionita, M. Hotspots for Warm and Dry Summers in Romania. *Nat. Hazards Earth Syst. Sci.* **2022**, *22*, 1347–1369. [CrossRef]
12. Russo, S.; Sillmann, J.; Fischer, E.M. Top Ten European Heatwaves since 1950 and Their Occurrence in the Coming Decades. *Environ. Res. Lett.* **2015**, *10*, 124003. [CrossRef]
13. Spinoni, J.; Lakatos, M.; Szentimrey, T.; Bihari, Z.; Szalai, S.; Vogt, J.; Antofie, T. Heat and Cold Waves Trends in the Carpathian Region from 1961 to 2010. *Int. J. Climatol.* **2015**, *35*, 4197–4209. [CrossRef]
14. United Nations—Department of Economic and Social Affairs. Goal15. Available online: <https://sdgs.un.org/goals/goal15> (accessed on 20 November 2022).
15. Gonzalez-Roglich, M.; Zvoleff, A.; Noon, M.; Liniger, H.; Fleiner, R.; Harari, N.; Garcia, C. Synergizing Global Tools to Monitor Progress towards Land Degradation Neutrality: Trends.Earth and the World Overview of Conservation Approaches and Technologies Sustainable Land Management Database. *Environ. Sci. Policy* **2019**, *93*, 34–42. [CrossRef]
16. Gemitzi, A.; Banti, M.A.; Lakshmi, V. Vegetation Greening Trends in Different Land Use Types: Natural Variability versus Human-Induced Impacts in Greece. *Environ. Earth Sci.* **2019**, *78*, 172. [CrossRef]
17. Zhong, L.; Ma, Y.; Xue, Y.; Piao, S. Climate Change Trends and Impacts on Vegetation Greening Over the Tibetan Plateau. *J. Geophys. Res. Atmos.* **2019**, *124*, 7540–7552. [CrossRef]
18. Wu, J.; Liang, S. Assessing Terrestrial Ecosystem Resilience Using Satellite Leaf Area Index. *Remote Sens.* **2020**, *12*, 595. [CrossRef]
19. Sims, N.C.; Green, C.; Newnham, G.J.; England, J.R.; Held, A.; Wulder, M.A.; Herold, M.; Cox, S.J.D.; Huete, A.R.; Kumar, L.; et al. *Good Practice Guidance: SDG Indicator 15.3.1. Version 1.0*; United Nations Convention to Combat Desertification: Bonn, Germany, 2017; pp. 1–115.
20. Cherlet, M.; Hutchinson, C.; Reynolds, J.; Hill, J.; Sommer, S.; von Maltitz, G. *World Atlas of Desertification*; Publication Office of the European Union: Luxembourg, 2018.
21. Kosmas, C.; Kirkby, M.; Geeson, N. *The Medalus Project Mediterranean Desertification and Land Use Manual on Key Indicators of Desertification and Mapping Environmentally Sensitive Areas to Desertification*; Kosmas, C., Kirkby, M., Geeson, N., Eds.; Office for Official Publications of the European Communities: Luxembourg, 1999; ISBN 92-828-6349-2.
22. Avram, S.; Corpade, A.M.; Corpade, C.; Croitoru, A.; Dedu, S.; Gheorghe, C.; Malos, C.V.; Manta, N.; Niculae, I.M.; Ontel, I.; et al. *Atlasul Ecosistemelor Degradate Din Romania*; Avram, S., Croitoru, A., Gheorghe, C., Eds.; Editura Academiei Române: Bucharest, Romania, 2021.
23. Avram, S.; Gheorghe, C.; Croitoru, A.; Bădărău, A.S.; Bărbos, M.; Burlacu, R.; Ciocănea, C.; Cipu, E.; Ciuiinel, A.; Corpade, A.-M.; et al. *Cartarea Ecosistemelor Naturale Si Seminaturale Degradate*; Avram, S., Croitoru, A., Gheorghe, C., Manta, N., Eds.; Romanian Academy: Bucharest, Romania, 2018.
24. Eskandari Dameneh, H.; Gholami, H.; Telfer, M.W.; Comino, J.R.; Collins, A.L.; Jansen, J.D. Desertification of Iran in the Early Twenty-First Century: Assessment Using Climate and Vegetation Indices. *Sci. Rep.* **2021**, *11*, 20548. [CrossRef]

25. Olsson, L.; Barbosa, H.; Bhadwal, S.; Cowie, A.; Delusca, K.; Flores-Renteria, D.; Hermans, K.; Jobbagy, E.; Kurz, W.; Li, D.; et al. Land Degradation. In *Climate Change and Land: An IPCC Special Report on Climate Change, Desertification, Land Degradation, Sustainable Land Management, Food Security, and Greenhouse Gas Fluxes in Terrestrial Ecosystems*; Shukla, P.R., Skea, J., Buendia, E.C., Masson-Delmotte, V., Pörtner, H.-O., Roberts, D.C., Zhai, P., Slade, R., Connors, S., Diemen, R., et al., Eds.; Intergovernmental Panel on Climate Change (IPCC): Geneva, Switzerland, 2019.
26. Cheval, S.; Popa, A.; Şandric, I.; Iojă, I. Exploratory Analysis of Cooling Effect of Urban Lakes on Land Surface Temperature in Bucharest (Romania) Using Landsat Imagery. *Urban Clim.* **2020**, *34*, 100696. [[CrossRef](#)]
27. Cui, Y.; Li, X. A New Global Land Productivity Dynamic Product Based on the Consistency of Various Vegetation Biophysical Indicators. *Big Earth Data* **2022**, *6*, 36–53. [[CrossRef](#)]
28. Lamchin, M.; Lee, J.-Y.; Lee, W.-K.; Lee, E.J.; Kim, M.; Lim, C.-H.; Choi, H.-A.; Kim, S.-R. Assessment of Land Cover Change and Desertification Using Remote Sensing Technology in a Local Region of Mongolia. *Adv. Space Res.* **2016**, *57*, 64–77. [[CrossRef](#)]
29. Tolche, A.D.; Gurara, M.A.; Pham, Q.B.; Anh, D.T. Modelling and Accessing Land Degradation Vulnerability Using Remote Sensing Techniques and the Analytical Hierarchy Process Approach. *Geocarto Int.* **2021**, *37*, 7122–7142. [[CrossRef](#)]
30. FAO. *Lesotho: Land Cover Atlas 2017–2021*; FAO: Maseru, Lesotho, 2023; ISBN 978-92-5-137412-2.
31. Ma, Y.J.; Shi, F.Z.; Hu, X.; Li, X.Y. Threshold Vegetation Greenness under Water Balance in Different Desert Areas over the Silk Road Economic Belt. *Remote Sens.* **2020**, *12*, 2452. [[CrossRef](#)]
32. Ibrahim, Y.Z.; Balzter, H.; Kaduk, J.; Tucker, C.J. Land Degradation Assessment Using Residual Trend Analysis of GIMMS NDVI3g, Soil Moisture and Rainfall in Sub-Saharan West Africa from 1982 to 2012. *Remote Sens.* **2015**, *7*, 5471–5494. [[CrossRef](#)]
33. Yengoh, G.T.; Dent, D.; Olsson, L.; Tengberg, A.E.; Tucker, C.J. *The Use of the Normalized Difference Vegetation Index (NDVI) to Assess Land Degradation at Multiple Scales: A Review of the Current Status, Future Trends, and Practical Considerations*; Springer: Berlin/Heidelberg, Germany, 2014; ISBN 9783319241128.
34. Fang, O.; Wang, Y.; Shao, X. The Effect of Climate on the Net Primary Productivity (NPP) of Pinus Koraiensis in the Changbai Mountains over the Past 50 Years. *Trees* **2016**, *30*, 281–294. [[CrossRef](#)]
35. Cowie, A.L.; Orr, B.J.; Castillo Sanchez, V.M.; Chasek, P.; Crossman, N.D.; Erlewein, A.; Louwagie, G.; Maron, M.; Metternicht, G.I.; Minelli, S.; et al. Land in Balance: The Scientific Conceptual Framework for Land Degradation Neutrality. *Environ. Sci. Policy* **2018**, *79*, 25–35. [[CrossRef](#)]
36. Eisfelder, C.; Klein, I.; Niklaus, M.; Kuenzer, C. Net Primary Productivity in Kazakhstan, Its Spatio-Temporal Patterns and Relation to Meteorological Variables. *J. Arid Environ.* **2014**, *103*, 17–30. [[CrossRef](#)]
37. Jung, M.; Reichstein, M.; Ciais, P.; Seneviratne, S.I.; Sheffield, J.; Goulden, M.L.; Bonan, G.; Cescatti, A.; Chen, J.; de Jeu, R.; et al. Recent Decline in the Global Land Evapotranspiration Trend Due to Limited Moisture Supply. *Nature* **2010**, *467*, 951–954. [[CrossRef](#)] [[PubMed](#)]
38. Cârlan, I.; Haase, D.; Große-Stoltenberg, A.; Sandric, I. Mapping Heat and Traffic Stress of Urban Park Vegetation Based on Satellite Imagery—A Comparison of Bucharest, Romania and Leipzig, Germany. *Urban Ecosyst.* **2020**, *23*, 363–377. [[CrossRef](#)]
39. Mirzabaev, A.; Wu, J.; Evans, J.; García-Oliva, F.; Hussein, I.A.G.; Iqbal, M.H.; Kimutai, J.; Knowles, T.; Meza, F.; Nedjraoui, D.; et al. Desertification. In *Climate Change and Land: An IPCC Special Report on Climate Change, Desertification, Land Degradation, Sustainable Land Management, Food Security, and Greenhouse Gas Fluxes in Terrestrial Ecosystems*; Shukla, P.R., Skea, J., Buendia, E.C., Masson-Delmotte, V., Pörtner, H.-O., Roberts, D.C., Zhai, P., Slade, R., Connors, S., Diemen, R., et al., Eds.; Intergovernmental Panel on Climate Change (IPCC): Geneva, Switzerland, 2019.
40. Angelopoulou, T.; Tziolas, N.; Balafoutis, A.; Zalidis, G.; Bochtis, D. Remote Sensing Techniques for Soil Organic Carbon Estimation: A Review. *Remote Sens.* **2019**, *11*, 676. [[CrossRef](#)]
41. Ladoni, M.; Bahrami, H.A.; Alavipanah, S.K.; Norouzi, A.A. Estimating Soil Organic Carbon from Soil Reflectance: A Review. *Precis. Agric.* **2010**, *11*, 82–99. [[CrossRef](#)]
42. Beck, H.E.; Zimmermann, N.E.; McVicar, T.R.; Vergopolan, N.; Berg, A.; Wood, E.F. Present and Future Köppen-Geiger Climate Classification Maps at 1-Km Resolution. *Sci. Data* **2018**, *5*, 180214. [[CrossRef](#)]
43. EEA. Copernicus Land Monitoring Service (Pan-European). Available online: <https://land.copernicus.eu/pan-european/corine-land-cover/clc2018?tab=mapview> (accessed on 11 May 2021).
44. NASA USGS MODIS. Available online: <https://modis.gsfc.nasa.gov/data/> (accessed on 10 December 2021).
45. Didan, K. MOD13A1 MODIS/Terra Vegetation Indices 16-Day L3 Global 500m SIN Grid V006 [Data set] NASA EOSDIS Land Processes Distributed Active Archive Center. 2015. Available online: <https://doi.org/10.5067/MODIS/MOD13A1.006> (accessed on 10 December 2021).
46. Running, S.; Mu, Q.; Zhao, M. MOD17A2H MODIS/Terra Gross Primary Productivity 8-Day L4 Global 500m SIN Grid V006 [Data set]. NASA EOSDIS Land Processes Distributed Active Archive Center. 2015. Available online: <https://lpdaac.usgs.gov/products/mod13a2v061/> (accessed on 10 December 2021).
47. Running, S.; Mu, Q.; Zhao, M. MOD16A2 MODIS/Terra Net Evapotranspiration 8-Day L4 Global 500m SIN Grid V006 [Data set]. NASA EOSDIS Land Processes Distributed Active Archive Center. 2017. Available online: <https://doi.org/10.5067/MODIS/MOD16A2.006> (accessed on 10 December 2021).
48. Wan, Z.; Hook, S.; Hulley, G. MOD11A1 MODIS/Terra Land Surface Temperature/Emissivity Daily L3 Global 1km SIN Grid V006. Available online: <https://lpdaac.usgs.gov/products/mod11a1v006/> (accessed on 16 August 2021).

49. Schaaf, C.; Wang, Z. MCD43A3 MODIS/Terra+Aqua BRDF/Albedo Daily L3 Global—500m V006 [Data set]. NASA EOSDIS Land Processes Distributed Active Archive Center. 2021. Available online: <https://doi.org/10.5067/MODIS/MCD43A3.006> (accessed on 10 December 2021).
50. UNCCD. *SDG Indicator 15.3.1*; United Nations Convention to Combat Desertification: Bonn, Germany, 2017.
51. Priyadharshini, R.; Radha, M.; Kumaraperumal, R.; Vanitha, G.; Kannan, B. Characterization of Environmental Covariates of Coimbatore District Using Principal Component Analysis. *Int. J. Curr. Microbiol. Appl. Sci.* **2021**, *10*, 3114–3123. [CrossRef]
52. Gilbert, R.O. *Statistical Methods for Environmental Pollution Monitoring*; Van Nostrand Reinhold Company Inc.: New York, NY, USA, 1987; ISBN 0442230508.
53. Mann, H.B. Nonparametric Tests Against Trend. *Econometrica* **1945**, *13*, 245–259. [CrossRef]
54. Abdi, H.; Williams, L.J. Principal Component Analysis. *WIREs Comput. Stat.* **2010**, *2*, 433–459. [CrossRef]
55. ESRI How Principal Components Works. Available online: <https://desktop.arcgis.com/en/arcmap/10.3/tools/spatial-analyst-toolbox/how-principal-components-works.htm> (accessed on 10 March 2023).
56. Fawcett, T. An Introduction to ROC Analysis. *Pattern Recognit. Lett.* **2006**, *27*, 861–874. [CrossRef]
57. Robin, X.; Turck, N.; Hainard, A.; Tiberti, N.; Lisacek, F.; Sanchez, J.-C.; Müller, M. PROC: An Open-Source Package for R and S+ to Analyze and Compare ROC Curves. *BMC Bioinform.* **2011**, *12*, 77. [CrossRef]
58. Nahm, F.S. Receiver Operating Characteristic Curve: Overview and Practical Use for Clinicians. *Korean J. Anesthesiol.* **2022**, *75*, 25–36. [CrossRef]
59. Maliva, R.; Missimer, T. *Geology of Arid Lands BT—Arid Lands Water Evaluation and Management*; Maliva, R., Missimer, T., Eds.; Springer: Berlin/Heidelberg, Germany, 2012; pp. 43–94. ISBN 978-3-642-29104-3.
60. Prăvălie, R. Climate Issues on Aridity Trends of Southern Oltenia in the Last Five Decades. *Geogr. Tech.* **2013**, *17*, 70–79.
61. Zomer, R.J.; Xu, J.; Trabucco, A. Version 3 of the Global Aridity Index and Potential Evapotranspiration Database. *Sci. Data* **2022**, *9*, 409. [CrossRef] [PubMed]
62. Greve, P.; Roderick, M.L.; Ukkola, A.M.; Wada, Y. The Aridity Index under Global Warming. *Environ. Res. Lett.* **2019**, *14*, 124006. [CrossRef]
63. Chai, R.; Mao, J.; Chen, H.; Wang, Y.; Shi, X.; Jin, M.; Zhao, T.; Hoffman, F.M.; Ricciuto, D.M.; Wulschleger, S.D. Human-Caused Long-Term Changes in Global Aridity. *npj Clim. Atmos. Sci.* **2021**, *4*, 65. [CrossRef]
64. Ord, J.K.; Getis, A. Local Spatial Autocorrelation Statistics: Distributional Issues and an Application. *Geogr. Anal.* **1995**, *27*, 286–306. [CrossRef]
65. ESRI How Hot Spot Analysis (Getis-Ord Gi\*) Works. Available online: <https://desktop.arcgis.com/en/arcmap/10.3/tools/spatial-statistics-toolbox/h-how-hot-spot-analysis-getis-ord-gi-spatial-stati.htm> (accessed on 15 January 2023).
66. Angearu, C.V.; Ontel, I.; Boldeanu, G.; Mihailescu, D.; Nertan, A.; Craciunescu, V.; Catana, S.; Irimescu, A. Multi-Temporal Analysis and Trends of the Drought Based on Modis Data in Agricultural Areas, Romania. *Remote Sens.* **2020**, *12*, 3940. [CrossRef]
67. Dobri, R.V.; Sfică, L.; Amihaesei, V.A.; Apostol, L.; Timpu, S. Arable Lands in Romania Derived from Normalized Difference Drought Index (2001–2020). *Remote Sens.* **2021**, *13*, 1478. [CrossRef]
68. Niacsu, L.; Bucur, D.; Ionita, I.; Codru, I.C. Soil Conservation Measures on Degraded Land in the Hilly Region of Eastern Romania: A Case Study from Puriceni-Bahnari Catchment. *Water* **2022**, *14*, 525. [CrossRef]
69. Niacsu, L.; Ionita, I.; Samoila, C.; Grigoras, G.; Blebea-Apostu, A.M. Land Degradation and Soil Conservation Measures in the Moldavian Plateau, Eastern Romania: A Case Study from the Racova Catchment. *Water* **2021**, *13*, 2877. [CrossRef]
70. Bilaşco, S.; Roşca, S.; Vescan, I.; Fodorean, I.; Dohotar, V.; Sestras, P. A GIS-Based Spatial Analysis Model Approach for Identification of Optimal Hydrotechnical Solutions for Gully Erosion Stabilization. Case Study. *Appl. Sci.* **2021**, *11*, 4847. [CrossRef]
71. Sestras, P.; Bilaşco, S.; Roşca, S.; Dudic, B.; Hysa, A.; Spalević, V. Geodetic and UAV Monitoring in the Sustainable Management of Shallow Landslides and Erosion of a Susceptible Urban Environment. *Remote Sens.* **2021**, *13*, 385. [CrossRef]
72. Patriche, C.V. Quantitative Assessment of Rill and Interrill Soil Erosion in Romania. *Soil Use Manag.* **2019**, *35*, 257–272. [CrossRef]
73. Marusca, T.; Oprea, A.; Memedemin, D.; Pop, O.G.; Ţibirnac, M.; Maftai, D.I.; Simion, I.; Taulescu, E. Assessment of Phytodiversity and Productivity of Steppic Grasslands from ROSCI0201 Podişul Nord-Dobrogean. *Delta Dunării* **2020**, *8*, 63–82.
74. Maruşca, T.; Memedemin, D.; Groza, A.; Pop, O.; Simion, I.; Taulescu, E. Comparative Study of Steppic Grasslands Productivity and Grazing Pressure in Babadag and Casimcea Plateaus. *Ann. Acad. Rom. Sci. Agric. Silv. Vet. Med. Sci.* **2019**, *8*, 33–42.
75. Cheval, S.; Dumitrescu, A.; Adamescu, M.; Cazacu, C. Identifying Climate Change Hotspots Relevant for Ecosystems in Romania. *Clim. Res.* **2020**, *80*, 165–173. [CrossRef]
76. Achim, E.; Manea, G.; Vijulie, I.; Cocoş, O.; Tarla, L. Ecological Reconstruction of the Plain Areas Prone to Climate Aridity through Forest Protection Belts. Case Study: Dăbuleni Town, Oltenia Plain, Romania. *Procedia Environ. Sci.* **2012**, *14*, 154–163. [CrossRef]
77. Fraser, E.D.G.; Stringer, L.C. Explaining Agricultural Collapse: Macro-Forces, Micro-Crises and the Emergence of Land Use Vulnerability in Southern Romania. *Glob. Environ. Chang.* **2009**, *19*, 45–53. [CrossRef]
78. Secu, C.V.; Stoleriu, C.C.; Lesenciuc, C.D.; Ursu, A. Normalized Sand Index for Identification of Bare Sand Areas in Temperate Climates Using Landsat Images, Application to the South of Romania. *Remote Sens.* **2022**, *14*, 3802. [CrossRef]
79. Vijulie, I.; Matei, E.; Manea, G.; Ţîrl, L.; Cuculici, R. Land Use Reconversion in the Drought—And Aridity—Affected Areas in SW Romania (Bechet, Dolj County). *Analale Univ. Bucurest Ser. Geogr.* **2017**, *1*, 69–81.

80. Kolecka, N. Greening Trends and Their Relationship with Agricultural Land Abandonment across Poland. *Remote Sens. Environ.* **2021**, *257*, 112340. [[CrossRef](#)]
81. Cho, M.A.; Ramoelo, A. Optimal Dates for Assessing Long-Term Changes in Tree-Cover in the Semi-Arid Biomes of South Africa Using MODIS NDVI Time Series (2001–2018). *Int. J. Appl. Earth Obs. Geoinf.* **2019**, *81*, 27–36. [[CrossRef](#)]
82. ANANP. Plan de Management Integrat Pentru Situl Natura 2000 ROSPA0135 Nisipurile de La Dăbuleni Și Aria Protejată de Interes Național 2.667 Casa Pădurii Din Pădurea Potelu. 2015. Available online: [http://www.mmediu.ro/app/webroot/uploads/files/2015-12-07\\_Plan\\_management\\_ROSPA0135\\_versiunea\\_2.pdf](http://www.mmediu.ro/app/webroot/uploads/files/2015-12-07_Plan_management_ROSPA0135_versiunea_2.pdf) (accessed on 15 January 2023).
83. ANANP. Limitele Ariilor Naturale Protejate. Available online: <http://www.mmediu.ro/articol/date-gis/434> (accessed on 15 January 2023).
84. World Bank Group. Promote Environmentally Sustainable Agriculture. Available online: <https://www.worldbank.org/en/topic/agriculture/brief/promote-environmentally-sustainable-agriculture> (accessed on 1 June 2023).
85. Satterthwaite, D.; McGranahan, G.; Tacoli, C. Urbanization and Its Implications for Food and Farming. *Philos. Trans. R. Soc. B Biol. Sci.* **2010**, *365*, 2809–2820. [[CrossRef](#)]
86. FAO. *The Future of Food and Agriculture—Trends and Challenges*; FAO: Rome, Italy, 2017.
87. Arima, E.Y.; Walker, R.T.; Perz, S.; Souza, C. Explaining the Fragmentation in the Brazilian Amazonian Forest. *J. Land Use Sci.* **2016**, *11*, 257–277. [[CrossRef](#)]

**Disclaimer/Publisher’s Note:** The statements, opinions and data contained in all publications are solely those of the individual author(s) and contributor(s) and not of MDPI and/or the editor(s). MDPI and/or the editor(s) disclaim responsibility for any injury to people or property resulting from any ideas, methods, instructions or products referred to in the content.